Prompt fission neutron investigation in $^{235}U(n_{th},f)$ reaction

Shakir Zeynalov[a], Pavel Sedyshev, Valery Shvetsov, and Olga Sidorova

Joint Institute for Nuclear Research, Frank Laboratory of Neutron Physics, 141980 Joliot-Curie 6, Dubna Moscow region, Russia

Abstract. The prompt neutron emission in thermal neutron induced fission of ^{235}U has been investigated applying digital signal electronics. The goal was to compare the results of this digital data acquisition and digital signal processing analysis to the results of the pioneering work of Apalin et al. Using a twin Frisch grid ionization chamber for the fission fragment detection and a NE213 equivalent neutron detector in total about 10^6 neutron coincidences have been registered. The fission fragment kinetic energy, mass and angular distribution has been investigated along with prompt neutron time of flight and pulse shape using a six channel synchronous waveform digitizer with sampling frequency of 250 MHz and 12 bit resolution. The signals have been analyzed using digital pulse processing algorithms, developed by authors. The thermal neutron beam was transported from the IBR-2 reactor to the target with bent mirror neutron guide.

1. Introduction

The nuclear fission is considered as the process of charged drop evolution under competition between attractive nuclear and repulsing coulomb forces, leading eventually to the split of the nucleus mainly into two parts of comparable masses. The main part of fission fragments (FF) excitation energy is released by the prompt fission neutrons (PFN), emitted by FF after full acceleration by coulomb forces. The experimental investigations of various characteristics of PFN emission is needed to understand the nuclear fission dynamics from the scission point down to rupture. One of the interesting observation is the increasing $\bar{\nu}(A)$ from the heavy fragment with increase of the excitation energy of the fissioning system [1] still has no clear explanation. Therefore, the need of further systematic studies of correlations between fragment and neutron characteristics is clear. The studies of PFN emission in fission induced by neutrons from energies extending from resonances up to a few MeV would contribute to better understanding the mechanism of PFN emission from the excited FF. The experiments on sub-barrier fission, induced by thermal neutrons are of particular interest because of no measurements was done so far on mass and energy distributions for this systems [2]. In this work we report preliminary results of PFN investigation thermal neutron-induced fission of ^{235}U. The first goal of the experiment was the feasibility check of the apparatus and data analysis procedure.

2. Experimental setup and FF data analysis procedure

A convenient way to study of PFN emission in neutron-induced fission is to use a conventional twin back-to-back ionization chamber, with two chambers sharing a common cathode as was done by Budtz-Jorgensen and Knitter [3]. The cathode is made from a thin conductive foil and at the same time serves as backing for the fissile deposit. For binary fission events two complementary FF are simultaneously detected in two independent chambers. Free electrons released by FF deceleration are induced pulses on the chambers anodes and on the common cathode during drift along the applied externally electric field. The pulse height in each chamber was proportional to corresponding FF kinetic energy release and the FF pulse shape conveys information on the FF angle (θ) in respect to the electric field applied in the direction of the normal to the cathode plane. From the correlated energies obtained in the above double-energy (2E) experiment, FF masses and velocities could be found in the way similar to that in book [4]. If the fissile target is located on the common cathode and the fast neutron detector positioned at the certain distance along the normal to the target the angle between FF and PFN emission would be equal to θ. The PFN velocity may be determined from the known flight path (0.65 m) and the measured time delay between cathode and ND pulses. Measured FF and PFN velocity vectors then may be used to reconstruct PFN emission kinematics. The PFN multiplicity distributions in respect to FF kinetic energy release and mass split may be reconstructed by comparison of two sets of FF measurements. In the first experiment fission fragment mass and kinetic energy release should be evaluated from the measurement independent from ND. In the second experiment FF mass and kinetic energy release should be evaluated for the FF coincided with ND. The detailed information on PFN emission in fission is available from the measured dependence of the number $\bar{\nu}(A, TKE)$ of PFN emitted by the FF with mass number A and TKE release of two fission fragments [3,4]. The $\bar{\nu}(A, TKE)$ function allows obtaining the averaged

$$\bar{\nu}(A) = \frac{\int_0^\infty \nu(A, TKE)Y(A, TKE)dTKE}{\int_0^\infty Y(A, TKE)dTKE} \quad (1)$$

[a] e-mail: zeinal@nf.jinr.ru

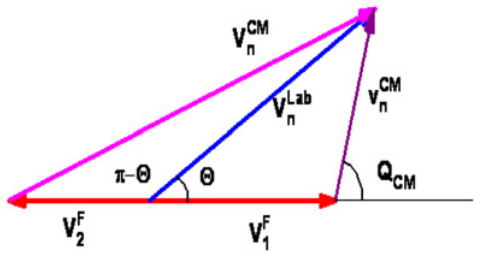

Figure 1. Vector diagram, depicts the PFN emission from the FF, where V_n^{CM}– is the velosity measured in CM of PFN, emitted by the complementary FF, v_n^{CM}, Θ – is the velosity and the emission angle in the LAB frame of FF moving toward the ND, V_n^{LAB} – the PFN velosity measured in the LAB frame. The Q_{CM} – the PFN emission angle, measured in the CM frame.

$$\bar{\nu} = \int_0^\infty \nu(A, TKE)Y(A, TKE)dTKEdA \quad (2)$$

$$200 = \int_0^\infty Y(A, TKE)dTKEdA \quad (3)$$

characteristics on $\bar{\nu}(A)$ or $\bar{\nu}(TKE)$ by integrating the $\bar{\nu}(A, TKE)$ over respective variable, if the mass yield matrix – *Y(A,TKE)* is known, then the integrating over A gives:

$$\bar{\nu}(TKE) = \frac{\int_0^\infty \nu(A, TKE)Y(A, TKE)dA}{\int_0^\infty Y(A, TKE)dA} \quad (4)$$

$$\bar{\nu} = \int_0^\infty \nu(A, TKE)Y(A, TKE)dTKEdA \quad (5)$$

$$200 = \int_0^\infty Y(A, TKE)dTKEdA \quad (6)$$

Similar relation could be written for averaging over the TKE. Functions $\bar{\nu}(A)$, $\bar{\nu}(TKE)$ can be easily determined if the distributions $\bar{\nu}(A, TKE)$ and $Y(A, TKE)$ are known. The experimental method and data analysis procedure implemented in this work was adopted from Ref. [3], where it was described in detail. For each fission event the FF and PFN kinetic energies, the FF masses along with the angle between PFN and FF motion should be determined. All this information can then be used to reconstruct the PFN emission kinematics both in the laboratory (LF) and in the centre of mass (CMF) frames. Reaction kinematics is sketched in the Fig. 1.

The experimental setup consisted of the twin back-to-back ionization chamber (TIC), which was designated for FF kinetic energy release and the cosine of angle between fission axis and the cathode plane normal measurement. The fissile target was made from enriched (99.99%) uranium vacuum evaporated on the polyamide foil with thickness of 35 μg/cm^2. The homogeneous uranium layer thickness was 48 μg/cm^2. The target was of circular shape with diameter of 70 mm, gold plated (∼20 μg/cm$^{2)}$ on the both side for electrical conductivity. TIC was operated with P10 gas mixture at constant flow (∼35 ml/min) at pressure of 1.05 bar. The experimental data was collected using a digital pulse processing (DPP) system, consisting of six synchronous waveform digitizers (12 bit, 250 MS/sec). The FF energies and angles were obtained from the chamber signal waveforms using DPP, realized in form

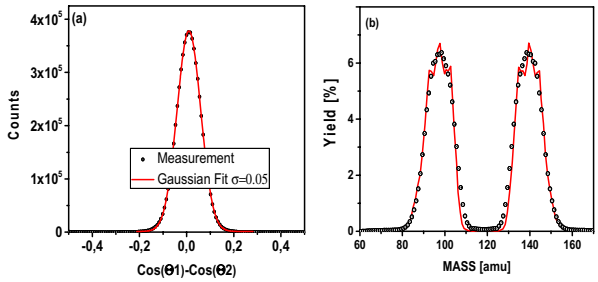

Figure 2. Demonstration of cos(θ) measurement quality (a) and the measured mass distribution with data from Ref. [4] p. 300 (b).

of recursive procedures. The neutron energy was derived from the time-of-flight (TOF) calculated as delay between the FF cathode and the neutron detector pulses. The measured energy release could be corrected for energy losses in the target layer and target backing if the cosine of angle θ is known. In this work anode current pulse waveform was derived from the output pulse of charge sensitive preamplifier and the pulse "centre of gravity" (T) calculated as described in Ref. [5]. The relation between T and the cos(θ) was derived in Ref. [6] using Ramo-Shockley theorem and numerically calculated weighting potentials:

$$\cos(\theta) = (T_{90} - T)/(T_{90} - T_0)$$
$$T_0 = T(\cos(\Theta) = 1), \mathrm{T}_{90} = T(\cos(\Theta) = 0) \quad (7)$$

The below formula was used to correct anode signal pulse heights for grid inefficiency:

$$P_A^C = P_A / \left(1 - \sigma\left(1 - \frac{T}{T_{90}}\right) \bullet \left(1 + \frac{d}{2D}\right)\right) \quad (8)$$

where the variables have the following meaning: D-is the cathode-anode distance, d-is the grid-anode distance, σ-is the Frisch grid inefficiency. Once the emission angle is calculated (accuracy of calculation is demostrated in Fig. 2a) the average anode pulse heights versus 1/cos(θ) value were plotted for both chambers to find energy loss correction for the FFs detected in each chamber. The data sets are fitted with linear functions of 1/cos(θ) and the evaluated slopes were assigned to energy loss correction in respective chamber. The correction for FFs pulse heights caused by momentum transfer to working gas atoms by FF (non ionizing collisions) during its deceleration – is called pulse height defect (PHD). The PHD depends on the FF mass and kinetic energy and was corrected in data analysis using parameterization suggested in Ref. [7]:

$$PHD(A_{post}, E_{post}) = \frac{A_{post} * E_{post}}{\alpha} + \frac{A_{post}}{\beta} \quad (9)$$

where the $E_{post}t$, A_{post} – are the FF kinetic energy and the mass after neutron emission. The fitting parameters α and β – are chosen to arrive at the values of TKE and $\langle A_H \rangle$ as given in Ref. [4] p. 323. After all corrections have been implemented the mass yield for investigated reaction was obtained. The $\bar{\nu}(A)$was taken from the Ref. [8].

For the pre-PFN emission FF mass calculations the successive approximation procedure described in Ref. [3] was used. The mass yield curve was obtained using $\bar{\nu}(A)$ from Ref. [8] is shown in Fig. 2(b) in comparison with

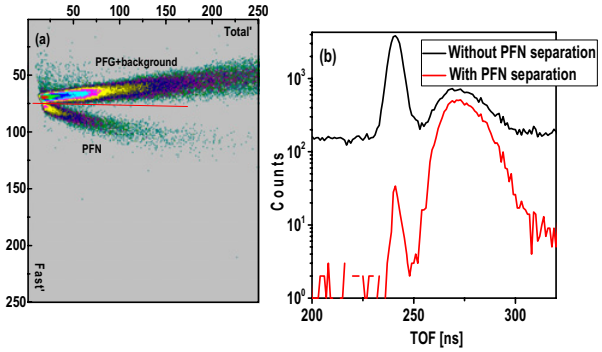

Figure 3. (a) Demonstration of pulse shape separation obtained with help of the two integral method along with (b) the PFN time-of-flight distribution before and after original signal.

result published in Ref. [4] p. 300. The FF kinetic energy was calculated using linear energy calibration scale with two parameters to set the TKE = 170.5 MeV and the light FF kinetic energy set to 100.6 MeV.

Measurement of PFN time-of-flight was done using cathode pulse of TIC as a "T-zero" signal and the ND signal as "Stop" signal. The signals were digitized with 250 MHz sampling rate and stored during experiment for further off-line analysis. Time difference between these two signals was analyzed implementing standard constant fraction time marking (CFTM) algorithm both to the cathode and to the ND waveforms. The copy of the original signal is delayed by approximately 0.4 of the cathode signal rise time (∼1000 ns) and summed with scaled and inverted pulse shape analysis applied and background was subtracted.

The "T-zero" time mark is assigned to the crossing point of resulting signal with time axis. The crossing point was calculated using parabola interpolation between two successive samples, first of which is positive and the second one is negative. The time mark for the ND signal was found in the similar way. It should be noted that to achieve the best timing resolution in CFTM realization one should convert sampled waveform to continuous form using Shannon's sampling formula [9]. Unless we did not deal with energy spectrum reconstruction, the resolution (∼2.5 ns) provided in this simple implementation was found sufficient for PFN analysis.

The neutron multiplicity is estimated by counting the number of coincidence between cathode pulse and PFN signal of ND. Due to high gamma radiation background both from the target and surrounding materials the PFN counts need to be separated (Fig. 3a,b) from the gamma radiation using pulse shape analysis as described in Ref. [9] p. 679. The PFN detected by ND is mainly emitted from FF moving towards the ND, but the probability, that it was emitted by FF moving in opposite direction (complementary FF) is not zero, and these events should be considered as background. In our research we implemented idea from Ref. [5] to evaluate the background from complementary FF fragment. According to the reaction kinematics depicted in Fig. 1 the kinetic energy of the PFN emitted by second (complementary) FF in the CMF, must be much higher than the kinetic energy of the PFN emitted from the first FF. Bearing in mind the exponential drop of the PFN energy spectrum in the CMF, the contribution to the PFN from both FFs could be

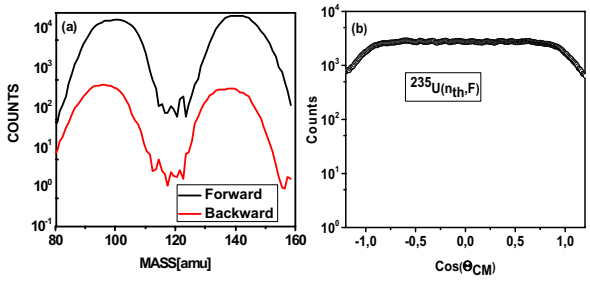

Figure 4. (a) Comparison of the background from the complementary FF to investigated PFN distribution. emission measured in the FF CM frame. (b) The angular distribution of PFN emission measured in the FF CM frame.

evaluated using the probabilities of PFN emission from the respective FF defined as:

$$W_1 = 1, \quad W_2 = \exp(E^1_{CM} - E^2_{CM}) \tag{10}$$

where W_1, W_2 – are probabilities of PFN emission with CM kinetic energies $E^{1,2}_{CM}$ of FF (with index 1) and its complement (with index 2) respectively. The relative PFN detection probabilities dependence on FFs mass values were evaluated and plotted in Fig. 4a. Result was similar to Ref. [3], where the background from the complementary fragment in ^{252}Cf(SF) was found to be small. The TOF range used in data analysis was measured relative to the maximum of the gamma peak. In our analysis the TOF range was 12<TOF<75 (ns), corresponding to the PFN energy range $0.37<E_n<11$ (MeV). The angular distribution of PFN emitted in FF CM reference frame was plotted in Fig. 4b, proving that almost all PFN was emitted from fully accelerated FFs. The transformation from the LAB to the CM reference frame was done using the following formula:

$$\int_0^\infty v_{CM} F(v_{CM}, \cos(\Theta_{CM}))dv_{CM} = \int_{V_L \cos(\Theta) > V_{FF}}^\infty v_L N(v_L, \cos(\Theta))dv \tag{11}$$

3. PFN distribution evaluation from the measured data

The PFN distribution was evaluated considering neutron emission from the fully accelerated FF and using the reference frame moving along with the FF towards the ND. We used the Jacobean factor and conversion formulae from CM to LAB reference frame from the Ref. [11] as follows:

$$\bar{\nu}(A, TKE) = \int_0^\infty \frac{Yc(A, TKE, V_{LAB}) \bullet V_{CM} \bullet (V_{LAB} - V_F \bullet \cos(\Theta))}{\varepsilon(V_{LAB}) \bullet V^2_{LAB}} \times dV_{LAB}/Y(A, TKE) \tag{12}$$

where $Y_C(A, TKE, V_{LAB})$ – the number of FF coincidences with ND, $\varepsilon(V_{LAB})$ – is the ND efficiency dependence on PFN velocity in LAB frame, V_{LAB} – the PFN velocity measured in LAB frame, V_F – FF fragment

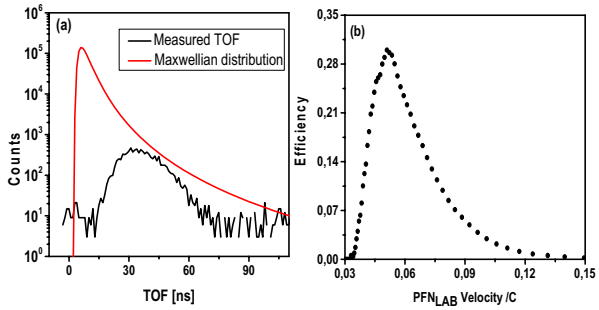

Figure 5. (a) Comparison of measured TOF with Maxwell distribution (kT=1.31 MeV, flight path=65 cm, 12<TOF< 75 [ns], 0.37<En<11 [MeV]) that was used to calculate the ND efficiency dependence on the PFN velocity (b).

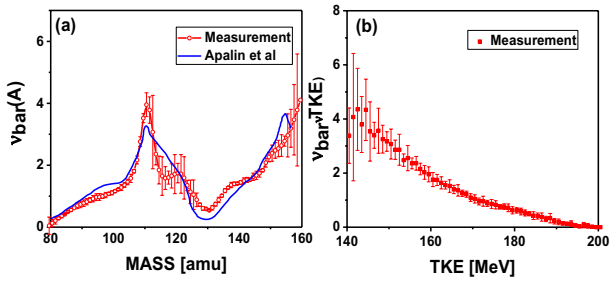

Figure 6. The FF Mass $\nu(A)$ (a) and the total kinetic energy $\nu(TKE)$ (b) dependence of the average PFN multiplicity obtained in reported measurement.

velocity in LAB frame, V_{CM} – is the PFN velocity in CM frame. The distribution $Y(A, TKE)$ calculated without demanding coincidence with ND as was described above, but distribution $Yc(A, TKE, V_{LAB})$ calculated with FF energy corrections as was described in Ref. [12].

4. Results and discussion

Comparison of measured in our experiment PFN multiplicity dependence on the FF mass with the result from Ref. [8], presented in Fig. 6(a), demonstrates some discrepancies. The error bars provided in our measurements are non-statistical, but calculated as the result obtained by averaging data from seven data sets, measured separately in different experiments. Each data set consisted of approximately $50*10^3$ FF coincidences with PFN detection. So the error bars demonstrate the scattering (beyond the statistical errors of results from different experiments. The most probable explanations of the result dispersion could be the background gamma radiation variations during the experiment. As the test of our result we compared pre-PFN emission mass yield curves, obtained from the common data set, analyzed using $\nu(A)$ data from our measurements and from the literature Ref. [8]. As it was mentioned earlier in this report, in data analysis procedure we used linear calibration procedure with two parameters: the light FF average kinetic energy (100.6 MeV) and the TKE (170.5 MeV). Result presented

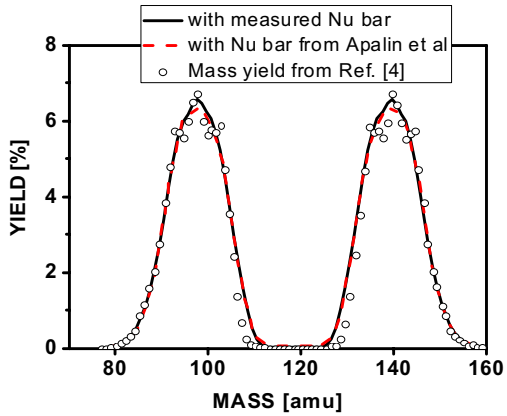

Figure 7. Comparison of pre-neutron mass yields obtained from the common data set. One was obtained using the $\bar{\nu}(A)$ measured in our experiment, another one with $\bar{\nu}(A)$ was taken from Ref. [8]. Mass yield curve from Ref. [4] was plotted (open circles) for reference.

in Fig. 7 (full line) obviously demonstrates better agreement with literature data (Ref. 4 p. 323) at the maximum of mass yield.

References

[1] A.A. Naqvi, F. Kappeler, and F. Dickmann, Phys. Rev. **C34**, 218 (1986)
[2] A. Al-Adili, D. Tarrio, F.-J. Hambsch, A. Gook, K. Jansson, A. Solders, V. Rakopoulos, C. Gustavson, M. Lantz, A. Materrs, S. Oberstedt, A.V. Prokofiev, M. Viladi, M. Osterlund, and S. Pomp, EPJ Web of Conferences **122**, 01007 (2016)
[3] C. Budtz-Jorgensen and H.-H. Knitter, Nucl. Phys. **A490**, 307 (1988)
[4] C. Wagemans, The Nuclear Fission Process, CRC Press, Boca Raton, FL, 1991
[5] Sh. Zeynalov, O. Zeynalova, F.-J. Hambsch and S. Oberstedt, Bull. Russ. Acad. Sci.: Phys. **73**, 506 (2009)
[6] Zeynalov Sh., Jaksybekov A., Sedyshev P., Sidorova O., Shvetsov V. **XXIV** International Seminar on Interaction of Neutrons with Nuclei, Dubna, May 23–27, 2016, JINR (to be published)
[7] F.-J. Hambsch, J. van Aarle, and R. Vogt, Nucl. Instrum. and Meth. **A361**, 257 (1995)
[8] V.F. Apalin, Yu. N. Gtitsuk, I.E. Kutikov, V.I. Lebedev, and L.A. Mikaelyan, Nucl. Phys. **55**, 249 (1964)
[9] O. Zeynalova, Sh. Zeynalov, M. Nazarenko, F.-J. Hambsch, and S. Oberstedt, AIP Conf. Proc. **1404**, 325 (2011)
[10] G. Knoll, Radiation Detection and Measurement, John Willey & Sons, Inc, Third edition, 2001
[11] H.R. Bowman, J.C.D. Milton, S.G. Thompson, and W.J. Swiatecki, Phys. Rev. **129**, 2133 (1963)
[12] A. Gavron, Nucl. Instrum. and Meth. **115**, 99 (1974)